Species-specific Differences among KCNMB3 BK β3 Auxiliary Subunits: Some β3 N-terminal Variants May Be Primate-specific Subunits

Xuhui Zeng, Xiao-Ming Xia, and Christopher J. Lingle

Department of Anesthesiology, Washington University School of Medicine, St. Louis, MO 63110

The KCNMB3 gene encodes one of a family of four auxiliary β subunits found in the mammalian genome that associate with Slo1 α subunits and regulate BK channel function. In humans, the KCNMB3 gene contains four N-terminal alternative exons that produce four functionally distinct β3 subunits, β3a–d. Three variants, β3a–c, exhibit kinetically distinct inactivation behaviors. Since investigation of the physiological roles of BK auxiliary subunits will depend on studies in rodents, here we have determined the identity and functional properties of mouse β3 variants. Whereas β1, β2, and β4 subunits exhibit 83.2%, 95.3%, and 93.8% identity between mouse and human, the mouse β3 subunit, excluding N-terminal splice variants, shares only 62.8% amino acid identity with its human counterpart. Based on an examination of the mouse genome and screening of mouse cDNA libraries, here we have identified only two N-terminal candidates, β3a and β3b, of the four found in humans. Both human and mouse β3a subunits produce a characteristic use-dependent inactivation. Surprisingly, whereas the hβ3b exhibits rapid inactivation, the putative mβ3b does not inactivate. Furthermore, unlike hβ3, the mβ3 subunit, irrespective of the N terminus, mediates a shift in gating to more negative potentials at a given Ca^{2+} concentration. The shift in gating gradually is lost following patch excision, suggesting that the gating shift involves some regulatory process dependent on the cytosolic milieu. Examination of additional genomes to assess conservation among splice variants suggests that the putative mβ3b N terminus may not be a true orthologue of the hβ3b N terminus and that both β3c and β3d appear likely to be primate-specific N-terminal variants. These results have three key implications: first, functional properties of homologous β3 subunits may differ among mammalian species; second, the specific physiological roles of homologous β3 subunits may differ among mammalian species; and, third, some β3 variants may be primate-specific ion channel subunits.

INTRODUCTION

Functional properties of Ca^{2+}-activated, large conductance BK-type K^+ channels are defined in part by the tissue-specific expression of auxiliary β subunits (Orio et al., 2002). Whereas the BK channel pore arises from the tetrameric assembly of four α subunits encoded by the single Slo1 gene (KCNMA1) (Butler et al., 1993; Salkoff et al., 2006), a family of four genes (KCNMB1–4; Orio et al., 2002) encodes the auxiliary β subunits available for coassembly into the BK channel complex. Such β subunits can also contribute in an up to 1:1 stoichiometry (Knaus et al., 1994; Wang et al., 2002) to the BK channel complex and play a critical role in defining many fundamental properties of BK channels. This includes the apparent Ca^{2+} dependence of channel activation (Cox and Aldrich, 2000), the tail current behaviors (Xia et al., 2000; Zeng et al., 2007), and the ability to inactivate (Wallner et al., 1999; Xia et al., 1999, 2000; Zeng et al., 2007). Both β1 and β2 subunits are able to shift the apparent Ca^{2+} dependence of gating (McManus et al., 1995; Wallner et al., 1999; Xia et al., 1999; Cox and Aldrich, 2000), such that at a given voltage, less Ca^{2+} is required for a given level of activation. Similarly, β4 subunits may also influence the Ca^{2+} dependence of activation over particular Ca^{2+} concentrations. β2 (Wallner et al., 1999; Xia et al., 1999) and some β3 (Uebele et al., 2000; Xia et al., 2000) subunits can produce inactivation that may regulate BK channel availability and BK tail current (Zeng et al., 2007). β4 may be the primary brain BK β subunit (Brenner et al., 2000a; Meera et al., 2000; Weiger et al., 2000), and has also been shown to influence some aspects of BK channel function and expression. Most of our understanding of the functional properties of the other auxiliary subunits stems largely from expression studies in heterologous systems, primarily using the human forms of the particular β subunits. However, our understanding of the roles of β1 and β4 subunits has been advanced considerably by the development of mice in which each of these subunits has been genetically removed (Brenner et al., 2000b, 2005). Our understanding of the roles of β2 and β3 subunits will most likely depend on similar approaches, and such studies may help provide insight into the physiological roles of inactivating BK channels.

In humans, there are four β3 splice variants that arise from four alternative exons each encoding a distinct N

Correspondence to Chris Lingle: clingle@morpheus.wustl.edu

The online version of this article contains supplemental material.

Abbreviation used in this paper: BK, large conductance Ca^{2+}-activated K^+ channel.

The Rockefeller University Press $30.00
J. Gen. Physiol. Vol. 132 No. 1 115–129
www.jgp.org/cgi/doi/10.1085/jgp.200809969

terminus (Uebele et al., 2000). Three of these are capable of mediating N-terminal–mediated inactivation of distinct temporal characteristics (Uebele et al., 2000; Xia et al., 2000; Zeng et al., 2007). Effects of the human β3 subunits on gating shifts appear to be minimal, except as a consequence of inactivation (Xia et al., 2000). Two of the β3 inactivating isoforms, β3a, and β3b, have been studied in some detail (Xia et al., 2000; Lingle et al., 2001; Zeng et al., 2007) and exhibit distinctive inactivation behaviors that presumably depend on the specific N-terminal sequences. Given that further exploration of the physiological roles of inactivating BK auxiliary subunits will certainly depend on investigations in mice or rats, here we have undertaken an examination of the identity and function of mouse BK β3 subunits. The results indicate that, in contrast to the four variants found in the human genome, the mouse genome encodes a single N-terminus, β3a, that is a clear homologue of a human variant. A second mouse variant similar to human β3b was also identified, but this appears to be of independent origin with distinct functional properties. We also undertook a comparison of conservation among β3 genes over a wide range of vertebrate species. This analysis suggests that β3b, β3c, and β3d may represent primate-specific genes. The analysis raises the possibility that β3 variants may have unique functions in primates and points out that the physiological roles of even homologous subunits may differ among species.

MATERIALS AND METHODS

Heterologous Expression of Cloned cDNAs in Oocytes

Stage IV *Xenopus laevis* oocytes were used for expression of currents as previously described (Xia et al., 1999, 2002). Slo1 α and β3 cRNA was typically prepared at ∼1 μg/μl, with Slo1 α cRNA diluted ∼1:40 before injection. The final standard ratio by mass of α:β3 RNA was ∼1:2.

Cloning and Generation of β3 Subunits

The preparation of human β3 subunits has been previously described (Xia et al., 2000). Mouse liver and testes cDNA libraries (Strategene) were used to screen for mβ3 variants using nested PCR. The first round PCR was performed with a LacZ reverse primer (5′GGAAACAGCTATGACCATG) and mβ3 primer (5′GAGCATGAAGGGCTTCAACACAGT). After a second round PCR with T3 primer and another mβ3 primer (5′CATCATGGCCACGCCCAGCAGCATGGC), the PCR products were analyzed with EcoRI and HINDIII and then subcloned into the pSK vector. 40 clones were analyzed and clone 39 corresponded to a β3b N terminus, with upstream residues corresponding to an open reading frame present within the mouse genome. This clone encoded a single methonione appended to exon 2 (primer sequence: lower case; putative exon 1b: underlined; exon 2: upper case; gaattcggcacgagg<u>GCAACTGCCACTCTGCAACGGCTTCCCACAACCCAGGGTTTCATGGATGCTTGGCAAACACTTTCCCAACAGAGGCTACCTCTCCAGTACCAGTATTCTACTTTAAAAAAAGATTTATTTT**AT**</u>GACAGCACTTCCGGCCTCGGGCAAAATCAATGGAGATCCCCTGAAGGTGCACCCAAAGCTT). The putative 1b transcript corresponds to position chr3:32,400,082-32,400,204 in the July, 2007 assembly of the mouse genome. In addition to this putative β3b N terminus, five other clones were obtained that contained putative reading frames appended to the shared β3 exon 2. Three (termed w, y, and z) of these did not encode an initiation methonine in the putative reading frame. Two others arose from different reading frames of the same region. One (putative Exon x1), corresponding to an open reading frame located 1,696 bp upstream of exon 1b, would result in an additional 42 N-terminal residues (MPVGRSKGVTSPRSFSATKS<u>VGVNLVYVGPRIDRERERWPDYV</u>). Only nucleotide sequence corresponding to the underlined translated residues was identified from cloning. The second (putative Exon x2) would result in addition of a single N-terminal methonine to exon 2, but with an alteration in the first residue following M such that the N terminus would begin MSLP instead of MTALP. No homologues corresponding to these sequences were found in a blast search of the human genome database and no rodent ESTs containing such N termini are present in current databases. A region of the rat genome shared homology with the putative exons x1 and x2, including a conserved GTGAGT intron–exon splice junction, but in the rat genome, the reading frame corresponding to exon x1 fails to encode an initiation methionine.

Mouse β3 subunits were generated by first cloning most of the β3 subunit (exons 2, 3, and 4) via PCR from the mouse liver cDNA library. Subsequently, β3a and β3b variants were generated by overlapping PCR from the 1a- and 1b-specific exons. Mutations of β3a and β3b subunits followed standard procedures in use in the laboratory (Xia et al., 2003; Zeng et al., 2003).

Electrophysiology

Currents were typically recorded in the inside-out configuration (Hamill et al., 1981) with an Axopatch 200 amplifier (Molecular Devices). For experiments with charybdotoxin, outside-out patches were employed. Voltage commands and data acquisition was accomplished with the Clampex program from the pClamp software package (Molecular Devices). The standard pipette/extracellular solution contained (in mM) 140 K-methanesulfonate, 20 KOH, 10 HEPES, 2 $MgCl_2$, pH 7.0. Gigaohm seals were formed while oocytes were bathed in frog Ringer (in mM, 115 NaCl, 2.5 KCl, 1.8 $CaCl_2$, 10 HEPES, pH 7.4). Patches were then excised into a flowing 0 Ca^{2+}, high K^+ solution. The composition of solutions bathing the cytoplasmic face of the patch membrane contained (in mM) 140 K-methanesulfonate (K-MES), 20 KOH, 10 HEPES. 5 mM EGTA was used for 0, 1, and 4 μM Ca^{2+} solutions, while 5 mM EGTA was used for 10 μM Ca^{2+} solutions. 60 and 300 μM Ca^{2+} solutions contained no added Ca^{2+} buffer. Solutions of defined Ca^{2+} were titrated to appropriate pCa with Ca-MES and calibrated against solutions of defined Ca^{2+} concentrations (World Precision Instruments) using a Ca^{2+}-sensitive electrode.

Solutions at the cytosolic face of membranes were controlled by a local application system containing six distinct perfusion lines. Each line was under independent solenoid control and solution flowed continuously from only one line at a time onto the excised patch. All experiments were at room temperature (∼22–25°C). Salts and CTX were obtained from Sigma-Aldrich.

Data Analysis

Analysis of current recordings was accomplished either with Clampfit (Molecular Devices) or with programs written in this laboratory. For families of G/V curves obtained within a patch, conductances were normalized to estimates of maximal conductance obtained at a Ca^{2+} concentration where a clear maximum was obtained. Individual G/V curves were fit with a Boltzmann function of the following form:

$$G(V) = \frac{G_{\max}}{1 + \exp^{\frac{-zF(V - V_h)}{RT}}}, \quad (1)$$

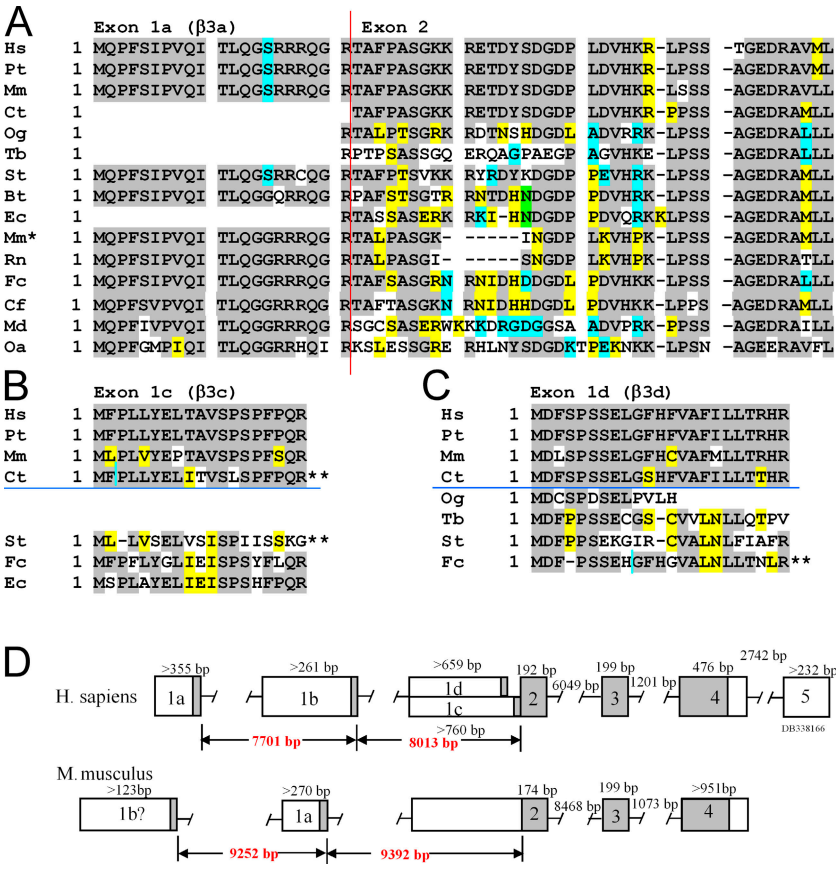

Figure 1. KCNMB3 N-terminal variation. (A) Predicted β3a (exon 1a) and the initial segment of exon 2 were determined for a range of vertebrate species from searches of publicly available databases, as described in the Materials and methods. Sequences are from the top: human (Hs: *Homo sapiens*), chimpanzee (Pt: *Pan troglodytes*), rhesus monkey (Mm: *Mulatta macaca*), marmoset (Ct: *Callithrix jacchus*), bushbaby (Og: *Otolemur garnettii*), treeshrew (Tb: *Tupaia belangeri*), thirteen-lined squirrel (St: *Spermophilus tridecemlineatus*), cow (Bt: *Bos taurus*), horse (Ec: *Equus caballus*), mouse (Mm': *Mus musculus*), rat (Rn: *Rattus norvegicus*), cat (Fc: *Felix catus*), dog (Cf: *Canus lupis familiaris*), opossum (Md: *Monodelphis domestica*), and duckbilled platypus (Oa: *Ornithorhynchus anatinus*). Exon 1a when attached to exon 2 encodes the β3a isoform. The β3b isoform is generated when exon 1b (not depicted), corresponding to a single methionine, is attached to Exon 2. Vertical red line indicates junction between N-terminal exons and exon 2. Gray highlights residues that are identical among most species. Unshaded residues are unique, while yellow, blue, or green indicate residues shared among a smaller subset of species. (B) Potential N termini with homology to human β3c are aligned. Horizontal blue line separates primate (above) and nonprimate (below) species. The marmoset (Ct) open reading frame (ORF) requires a change in reading frame (indicated by **), while the cat (St) ORF is in a different reading from exon 2. (C) Potential N termini with homology to human β3d are aligned with a horizontal blue line separating primates from other mammals. The cat putative β3d N terminus contained frame shifts and stop codons in the reading frame (**). (D) KCNMB3 gene maps for human and mouse are compared. In contrast to human, the putative mouse 1b coding exon (1b?) that was identified by cloning is positioned upstream of the conserved 1a exon.

where G_{max} is the fitted value for maximal conductance at a given Ca^{2+}, V_h is the voltage of half maximal activation of conductance, and z reflects the net charge moved across the membrane during the transition from the closed to the open state.

Genome Searches

For many of the genomes examined, gene assembly remains incomplete and annotation of the KCNMB genes is not available. Our examination of conservation within the KCNMB3 gene occurred in two passes. First, we used default BLAST settings using tblastn to search for known β subunit sequences. Second, we used the capabilities of the University of California-Santa Cruz Genome Bioinformatics website (www.genome.ucsc.edu; Kent et al., 2002) to obtain measures of conservation among various species within the presuming coding regions of the KCNBM3 N-terminal splice variants.

Tblastn searches typically returned regions of strong identity that reflect likely exons. Such exons were then assembled into the putative full subunit based on alignments with the validated β subunits. Sequence information for some genomes remains incomplete and, in some cases where genomes have only been sequenced at low coverage, sequencing errors may persist in the available databases. Tblastn searches were conducted on a number of genomes accessible from the www.ncbi.nlm.nih.gov/blast web page (chimp, rhesus monkey, cow, horse, cat, dog, mouse, rat, possum, platypus), additional genomes accessible from Ensembl (www.ensembl.org) release 47 web page (squirrel, bushbaby, tree shrew) and also the marmoset genome-sequencing project webserver (http://genome.wustl.edu/genome.cgi?GENOME=Callithrix%20jacchus). Mammalian genomes considered include human (*Homo sapiens*), chimpanzee (*Pan troglodytes*), rhesus monkey (*Mulatta macaca*), marmoset (*Callithrix jacchus*), bushbaby (*Otolemur garnetti*), tree shrew (*Tupaia belangeri*), thirteen-lined ground squirrel (*Spermophilus tridecemlineatus*), cow (*Bos taurus*), horse (*Equus caballus*), mouse (*Mus musculus*), rat (*Rattus norvegicus*), cat (*Felis catus*), dog (*Canis lupis familiaris*), opossum (*Monodelphis domestica*), and duck-billed platypus (*Ornithorhynchus anatinus*).

For the comparison of conservation using the UCSC genome browser (Kent et al., 2002), segments of putative human or rodent KCNMB3 exons were used to extract potentially homologous segments from other species. For searches for homologues of exon 1b sequences, the BLAT search was used (Kent, 2002). Aligned segments were examined visually for evidence of a GT base sequence at the donor splice site. PhastCons estimates of conservation (Siepel et al., 2005) were made both on a 28 species set of vertebrates and an 18 species set of placental mammals (human, chimp, rhesus, bushbaby, treeshrew, mouse, rat, guinea pig, rabbit, shrew, hedgehog, dog, cat, horse, cow, armadillo, elephant, tenrec); the placental mammal scores were used for display purposes. PhastCons scores are calculated based on a probabilistic model (two-state phylogenetic hidden Markov model) that considers the likelihood of DNA substitution at any position and the way this changes from one position to another (Siepel et al., 2005).

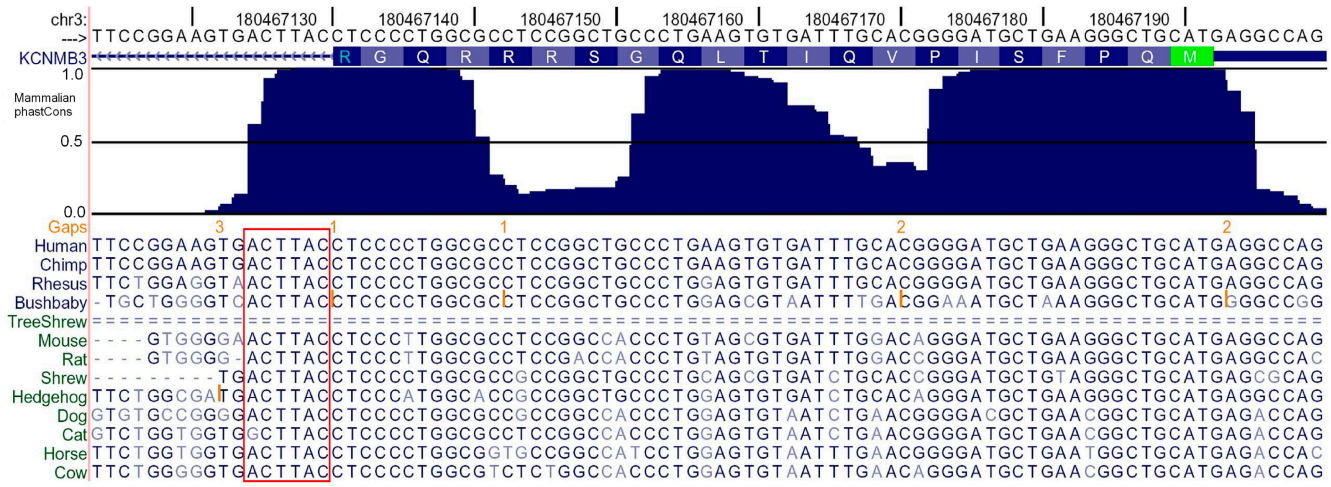

Figure 2. The KCNMB3 1a exon is highly conserved in mammals. Segments of nucleotides spanning the putative 1a exon of various placental mammals were aligned using the UCSC genome browser. Displayed nucleotides are complementary to those for mRNA and are displayed in reverse order to that typically used for amino acid alignments. The top two tracks show, respectively, the nucleotide positions on human chr. 3 and the presumptive open reading frame for the identified human 1a exon. The PhastCons plot shows scores for 17 placental mammals plus human over this genome segment. For the alignments, the segment boxed in red indicates the highly conserved consensus GT intron–exon splice site preceding the ORF (reverse complement: GTAAGT). Numbers on the Gaps track indicate number of inserted residues for particular species indicated by vertical orange lines. Double lines indicate segments with one or more unalignable bases. Single lines indicate positions with no alignable bases.

Scores reflect evolutionary distances among species, a model of the nucleotide substitution process, and a tendency for correlations in conservation levels to be found among adjacent sites in a genome.

For species in which specific annotation is available, GenBank/EMBL/DDBJ nos. are as follows: human, NM_171828; chimp, XM_001167560 (predicted); mouse, XM_912348 (predicted); rat, AB297662(EST).

Online Supplemental Material

The paper refers to eight supplemental figures (available at http://www.jgp.org/cgi/content/full/jgp.200809969/DC1) that provide additional information about β subunit sequence alignments (β3, Fig. S1; β1, Fig. S2; β2, Fig. S3; β4, Fig. S4), information about exon maps for various species (Fig. S5), translations in multiple reading frames for multiple species of the segments adjacent to exon 2 (Fig. S6), and homologies in N-terminal inactivation domains for Kv β (Fig. S7) and α (Fig. S8) subunits.

RESULTS

Putative β3 Sequences Exhibit Substantial Diversity Among Species

Alignment of a set of largely complete β3 amino acid sequences, either validated or predicted, is provided in Fig. S1 (available at http://www.jgp.org/cgi/content/full/jgp.200809969/DC1). Candidate β1, β2, and β4 sequences are also provided in Figs. S2–S4, respectively. Here we confine comparisons to mammalian β subunits, although it should be noted that most β subunits appear to have representatives in chicken, lizard, frog, and fish. The β3 sequences exhibit substantially more amino acid variation than observed for any of the other β subunits.

Identification of Potential Mouse β3 N-terminal Splice Variants from Database Searches and Cloning

The mouse genome was searched for sequences that exhibit homology to the four human β3 N-terminal splice variants. Sequence corresponding to a β3a N terminus (exon 1a; see Fig. 1 D for gene map) was readily identified (Fig. 1 A). Furthermore, a rat β3a EST (AB297662) was found in the public database supporting the view that this is an expressed sequence. Examination of multiple genomes revealed that the β3a N terminus is highly conserved in mammalian genomes (also see Fig. 2). The β3a N terminus is, in fact, one of the more highly conserved parts of the entire β3 subunit.

The β3b N terminus (exon 1b), when appended to the shared common exon 2 of the β3 gene, encodes only a single amino acid, methionine; naturally, the 1b exon is unrecognizable from tblastn searches. To test for the existence of a β3b variant in mice, we screened mouse liver and testes cDNA libraries for β3 subunit N termini (see Materials and methods). In humans, these tissues have been reported to express β3b, β3c, β3d message (Uebele et al., 2000). This screening resulted in identification of a clone that encoded a single initiation methonine appended to the shared exon 2, suggesting that a putative β3b homologue may be present in mouse tissues. The position of the putative β3 1b exon was identified in the mouse genome and found upstream of the other KCNMB3 exons, although with its position reversed relative to exon 1a in comparison to the human arrangement (Fig. 1 D). No other clones were identified that corresponded to any of the identified human N-terminal variants. However, as noted in the Materials

and methods, in some clones, additional sequences were found to be appended to exon 2 and corresponded to reading frames also found in the mouse genome upstream of the other KCNMB3 exons. The significance of such clones is unclear and is a subject of current investigation.

Finally, using a tblastn search of genomic and EST databases, no homologues of β3c or β3d were identified in either mouse or rat genomes, although some weak homologues were identified in other genomes (Fig. 1, B and C). All such homologues mapped to appropriate positions within the KCNMB3 genes (see Fig. S5). In sum, these considerations establish that a candidate β3b message is generated in mouse and that an exon encoding a β3a N terminus is present in the mouse genome. KCNMB3 1c and 1d exons are clearly not present in either mouse or rat genomes for which sequencing is thought to be largely complete.

The potential significance of the differences in the presence or absence of β3b, β3c, and β3d variants among species will be considered in more detail below. Furthermore, we present a comparison of the functional differences between the two candidate mouse KCNMB3 N-terminal exons, 1a and 1b, and their human counterparts.

The β3 1a Exon Is Highly Conserved among Mammals

Fig. 1 A showed that the 1a exon appears to be highly conserved among mammals, thereby suggesting that this gene region may provide a potential quantitative benchmark for expected strong conservation. The 1a exon region of the KCNMB3a gene was therefore analyzed with the conservation analysis features of the UCSC genome browser (Kent et al., 2002; Siepel et al., 2005). Fig. 2 illustrates nucleotide alignments along with PhastCons scores for a set of 17 placental mammals along with human (see Materials and methods). The complementary nucleotide sequences are displayed and presented in an order reversed from that used for amino acid alignments. The 1a exon exhibits strong conservation (PhastCons scores > 0.5) over most of its length and also contains a highly conserved canonical 5′ GT intron–exon splice donor site. These considerations support the view that there is strong selective pressure that has maintained the KCNMB3 1a exon within mammals.

Despite the strong conservation among β3a N termini, the segment of the shared exon 2 of the β3 N terminus that precedes the β3 subunit first transmembrane segment (TM1) exhibits substantial sequence variability (see Fig. 1 A) that might impact on the function of these subunits. We therefore compared the properties of human and mouse β3a subunits. A novel property of the hβ3a subunit is its ability to produce an inactivation-dependent enhancement of net tail current flux (Zeng et al., 2007). Similar to hβ3a subunits, coexpression of α with mβ3a subunits resulted in inactivating currents

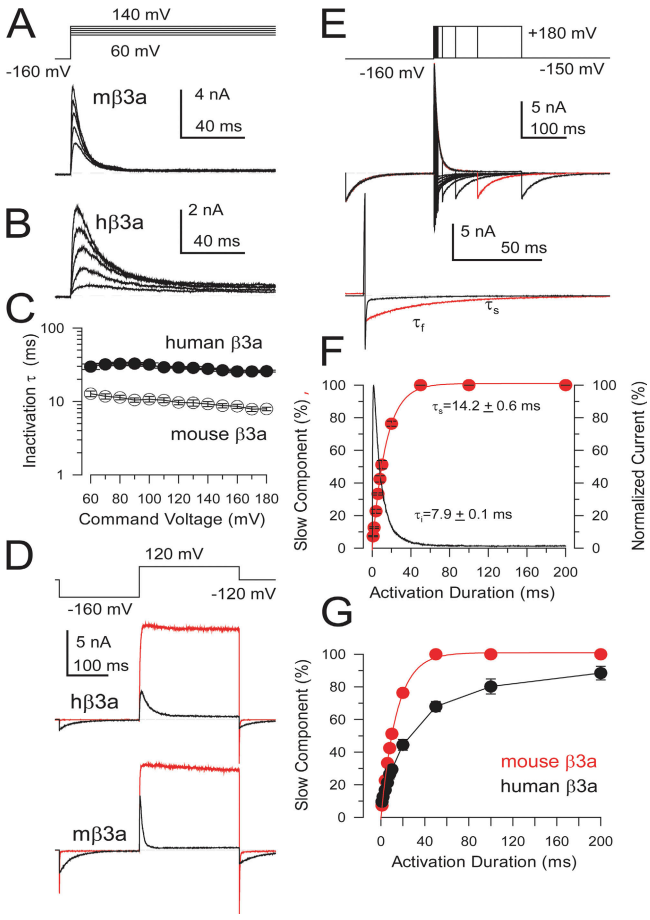

Figure 3. The mouse β3a subunit produces a use-dependent tail current enhancement similar to hβ3a, but mβ3a inactivation is more rapid and more complete. (A) Currents arising from α+mβ3a subunits were activated by the indicated protocol. (B) Currents resulting from α+hβ3a subunits show slower and more incomplete inactivation. Currents in both A and B were activated by the indicated voltage protocols with 10 μM cytosolic Ca^{2+}. (C) Inactivation time constants measured over a range of potentials are displayed for both hβ3a and mβ3a. (D) Currents arising from channels containing either mouse β3a subunits (top) or human β3a subunits (bottom) are displayed on a slower time base to emphasize the slow tail currents. Currents were activated by the indicated voltage protocol with 10 μM Ca^{2+}. Control currents are in red, while currents following brief application of 0.1 mg/ml trypsin are in black. Trypsin removes inactivation and the slow tail currents. (E) Activation steps of differing duration to +180 mV were used to elicit α+mβ3a currents with 10 μM Ca^{2+}. As the command step duration is increased, the tail current switches from exclusively fast deactivating to slow deactivating. Intermediate duration command steps elicit tail currents containing distinct slow and fast time constants. Below, a brief (black, τ_f) and more prolonged (red, τ_s) step are compared emphasizing the differences in tail currents in each case. (F) The fraction of slow time constant (τ_s: red circles) as a function of command step duration is plotted along with the time course of inactivation onset, showing the close correlation of the two. In G, the temporal development of the slow component of tail current is compared for mouse (red circles) and human (black circles) β3a subunits.

Figure 4. Primate and candidate rodent KCNMB3 1b exons probably arose independently and neither appear to be conserved among mammals. In A, the indicated genomes were compared using the UCSC genome browser for homologies to a segment from the cloned human KCNMB3 1b exon (Uebele et al., 2000) but also including 10 bases preceding the beginning of the presumed 1b ORF. Segments of homology are only observed in chimp and rhesus monkey, both of which also share a consensus sequence (red box) appropriate for an intron–exon junction just preceding the ORF. In B, the indicated genomes were compared for segments homologous to the 122 base pairs in the cloned putative mouse 1b exon, with no segments of homology found in any other mammalian genome. The candidate mouse 1b exon is preceded by an appropriate intron–exon splice site.

(Fig. 3). mβ3a subunits (Fig. 3 A) cause somewhat faster and more complete inactivation than hβ3a (Fig. 3, B and C). Whereas for hβ3a, persistent noninactivating current at +100 mV was 5.6 ± 0.6% (n = 3) of the maximal peak hβ3a current (measured after removal of inactivation by trypsin), for mβ3a the persistent current was 2.1 ± 0.3% (n = 6) of the maximum current. On average, mβ3a subunit results in about threefold faster inactivation than the human subunit (Fig. 3 C). Both subunits produce a characteristic inactivation-dependent slow tail current that is removed by digestion of the N terminus with trypsin (Fig. 3 D). The slow, use-dependent tail current appears to be the key functional property defined by the highly conserved β3a exon.

Given the differences in the inactivation time course mediated by hβ3a and mβ3a subunits, we also compared the time course of onset of the slow use-dependent tail currents. The development of the slow tail current component is dependent on the development of inactivation for both hβ3a and mβ3a (Fig. 3, E and F), with brief activation steps resulting in fast tail current deactivation and prolonged inactivating steps resulting in an exclusively slow tail current decay. The time course of development of the slow tail current mirrored the time course of inactivation (Fig. 3 F) and the faster inactivation rate of mβ3a channels resulted in a faster onset of the slow tail current in comparison to hβ3a (Fig. 3 G).

1b-Type Exons May Have Arisen Independently in Primates and Rodents, and May Be Absent in Other Species

Although we were able to clone a mouse 1b homologue, several factors raise some uncertainty as to whether the 1b homologue reflects a valid subunit variant. First, the position of the cloned candidate mouse 1b exon relative to the 1a exon was reversed in comparison to humans, suggesting that the putative mouse 1b exon may be of independent origin (Fig. 1 D). Second, because cloning revealed additional N-terminal sequences of unknown origin (see Materials and methods), some caution is warranted regarding the origins of the candidate 1b clone.

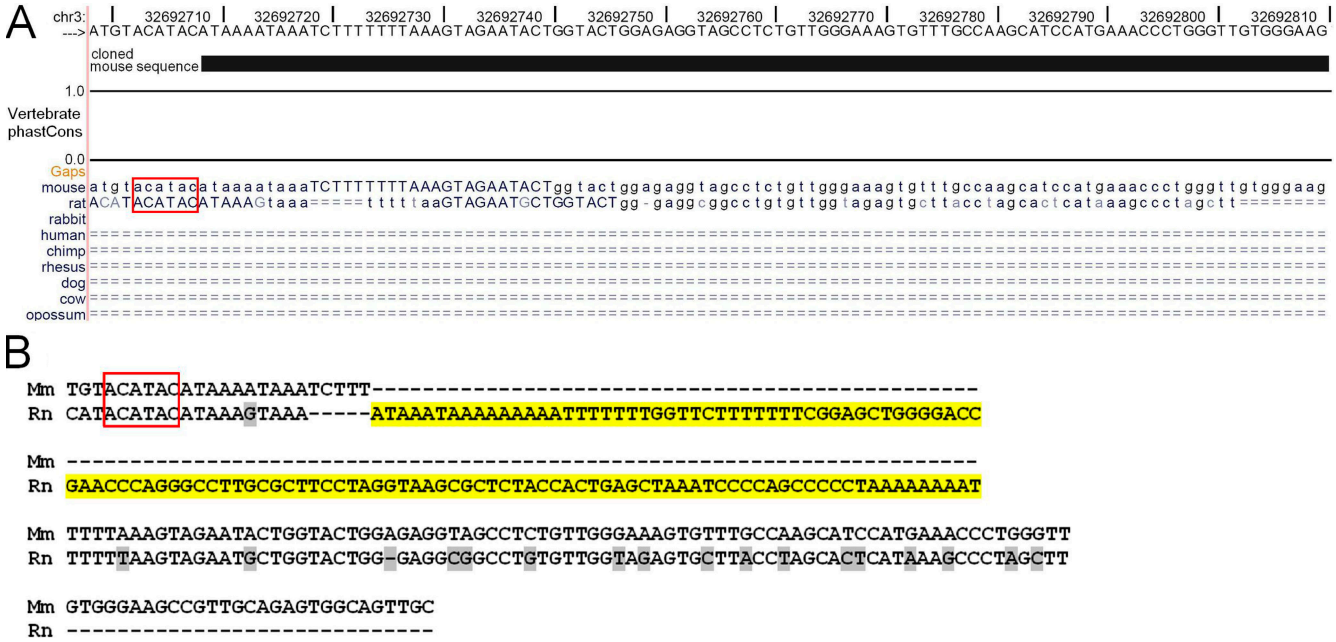

Figure 5. The rat genome contains a potential homologue of the mouse KCNMB3 1b' exon. (A) A lower stringency conservation screen, using the candidate mouse KCNMB3 1b' sequence (build mm8), identified a segment of potential homology in the rat. The rat segment contains a 120-bp insert of no homology that connects two segments sharing homology with the mouse 1b' exon. This rat 1b' homologue occurs in a position similar to that in the mouse within the overall KCNMB3 gene map (Fig. S5). (B) The cloned mouse 1b' exon is aligned directly with the candidate rat 1b' exon highlighting the insert (yellow) in the rat sequence. Both candidate exons share a similar consensus sequence for an appropriate intron–exon splice site. The 120-bp insert appears to be a repeatable genetic element occurring on multiple chromosomes in the rat. A homologue of ~90% identity is also found in the mouse. The position of the mouse 1b exon is, in build mm8, chr3:32,400,082-32,400,204, while in build mm8, the position is chr3:32,692,709-32,692,831. Alignments based on mm8 use a 17-way vertebrate species set while alignments based on mm9 use a 30-way Multiz alignment. The UCSC alignment procedures use an additional filtering step in the generation of the 30-way conservation track that reduces the number of paralogues and pseudogenes from the high-quality assemblies.

Third, the upstream noncoding sequence of the candidate 1b mouse segment exhibits minimal homology to that in humans. To further compare the putative 1b exons in both human and mouse, here we have examined the extent of conservation in nucleotides near human and mouse candidate 1b exons. If 1b exons contribute to expressed proteins that are conserved among sets of species, selective pressures should be acting upon the β3b subunits. In such cases, one might expect that there would be some conservation among genomes both in the intron–exon junction preceding the 1b exon and in its noncoding region.

A 200-bp segment of nucleotides corresponding to the noncoding sequence upstream of the human 1b ORF was compared against other genomes (Fig. 4 A), revealing a similar segment in both chimp and rhesus monkey. Other mammalian genomes did not reveal any homologous segment. All three primate genomes shared an appropriate canonical 5′ GT intron–exon splice donor site (GTAAGT; reverse complement). In contrast, when the 123 base pairs identified in the cloned candidate mouse 1b sequence were compared (using the mm9 mouse genome build) against genomes of other placental mammals, no homologues were identified (Fig. 4 B), although the candidate mouse 1b exon was preceded by an appropriate intron–exon 5′ splice donor site.

We also screened with the mouse 1b exon using build mm8 of the mouse genome. Alignments based on mm8 use a less restrictive filter for defining alignments than the mm9 build (www.genome.ucsc.edu). Stronger filtering tends to remove paralogues and pseudo-genes, but may also remove relevant orthologues of weaker homology. In this case, a region of homology was identified in the rat genome (Fig. 5 A). This corresponded to two distinct segments of homology, an initial 10 homologous residues adjacent to the presumed intron–exon splice site and then an additional segment of 78 bp of high homology, separated by a 120-bp insert in the rat genome (Fig. 5 B). Both genomes share similar consensus sequences denoting a canonical GT intron–exon splice donor site. Although this rat sequence is not recognized with homology screens based on the current build of the mouse genome, we think it likely that these are true orthologues. Both putative exons map to similar positions within their respective KCNMB3 gene maps (Fig. S5). It should be noted that the insert in the rat KCNMB3 gene region (Fig. 5 B) appears to be a transposable element, since blast searches of the rat genome

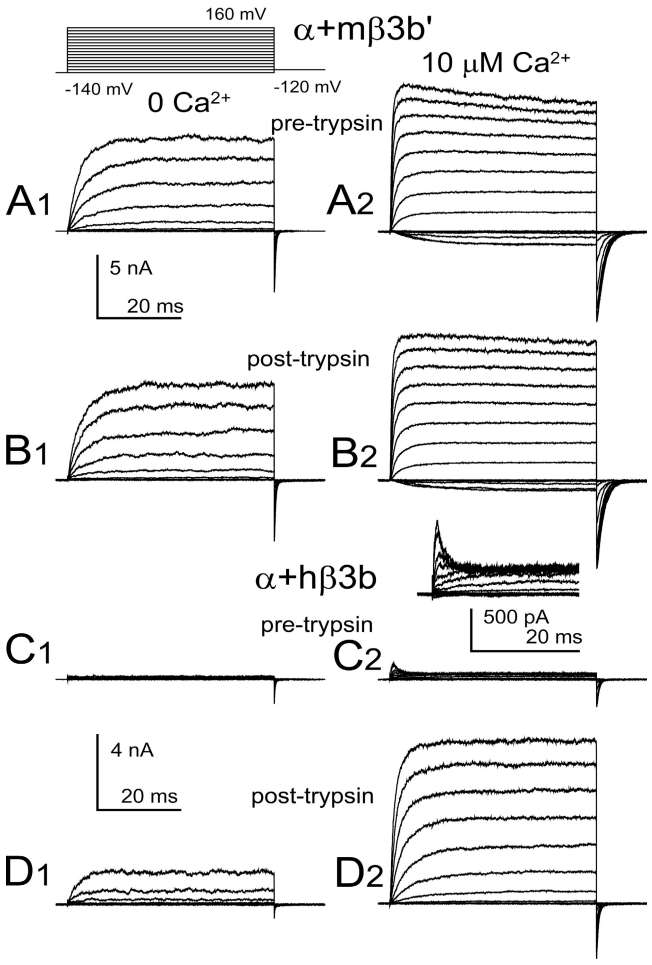

Figure 6. The mouse candidate β3b' subunit is functionally distinct from the human β3b subunit, failing to produce trypsin-sensitive inactivation of outward current. (A) Currents from α+mβ3b' subunits were activated with the indicated voltage protocol either with 0 (A1) or 10 (A2) μM cytosolic Ca^{2+}. (B) Currents were acquired from the same patch after application of 0.5 mg/ml trypsin for a period sufficient to remove inactivation mediated by hβ3b subunits. (C) Currents resulting from α+hβ3b subunits are displayed, with the inset in C2 showing currents at 10 μM at higher magnification to show the rapid inactivation at positive command potentials. (D) After application of trypsin, α+hβ3b currents are markedly increased both at 0 (D1) and 10 (D2) μM, due to removal of fast block at positive activation potentials.

reveal similar segments of almost complete identity on chrs. 1–20 and chr. X. This insert shows no conservation with any bacterial or viral genomic sequences. A similar repetitive element of >90% identity also appears in the mouse genome. Although these considerations provide some support to the idea that both mouse and rat contain an orthologous 1b exon, they do not allow a definitive conclusion regarding the validity of the 1b exon without explicit examination of expression of 1b message or protein.

The absence of homology between the primate and rodent 1b candidates and the differing relative positions on the KCNMB3 gene maps clearly suggest that the primate and rodent exons arose independently. We show below that subunits arising from the 1b exon in human and mouse produce markedly different functional effects, primarily because of differences between the N-terminal portions encoded by the shared exon 2. As such, to indicate that these two variants are not true orthologues, we will now refer to the mouse exon as 1b' and the expressed mouse subunit as β3b'.

Unlike hβ3b, the Putative mβ3b' Subunit Does Not Cause Inactivation of BK Current

The hβ3b subunit produces BK currents that exhibit rapid, but incomplete inactivation (Xia et al., 2000; Lingle et al., 2001). In contrast, coexpression of the putative mβ3b' subunit with mSlo1 α subunits resulted in currents that did not show time-dependent inactivation (Fig. 6 A). To test for the possibility that a very rapid inactivation process may be masking any visible time-dependent inactivation, trypsin was applied to the cytosolic face of such patches. No increase in outward current amplitude was observed (Fig. 6 B). These effects contrast markedly to the behavior of the human β3b subunit (Fig. 6, C and D).

The mβ3b' N terminus differs in two primary ways from the human β3b subunit. First, a hydrophobic phenylalanine residue, F4, at the beginning of the human β3b N terminus, is replaced by a leucine in mβ3b'. A critical role of bulky hydrophobic residues in inactivation has previously been demonstrated for the β2 N terminus (Xia et al., 2003). Second, the mβ3b' N terminus contains a six-residue deletion that may also impact on the ability of the N terminus to reach an appropriate blocking position. Although the length of the mβ3b' N terminus is sufficient to support inactivation in artificial N termini containing a three-residue inactivation segment and a polyglutamine linker (Xia et al., 2003), the combination of a weaker binding epitope (e.g., MTAL) coupled with shorter length might both contribute to the absence of inactivation. Three separate constructs were examined to test these ideas.

Two alterations were made in hβ3b in an attempt to make it more like mβ3b'. Construct hβ3b-F4L produced no observable time-dependent inactivation (Fig. 7 B) using protocols that reveal fast inactivation with wild-type hβ3b (see Fig. 7 A). However, application of trypsin resulted in pronounced increases in the outward current activated at positive potentials, indicative that the MTAL N terminus was still able to produce some block of the channel. However, the trypsin-mediated increase in current was much less than is observed for wild-type hβ3b (Fig. 7 A), indicative that the F4L mutation does weaken block by the β3 N terminus. In a second construct, hβ3b-Δ10-15, a deletion of six residues resulted in currents that showed a slight hint of time-dependent inactivation, but only at the most positive activation potentials (Fig. 7 C). However, the currents

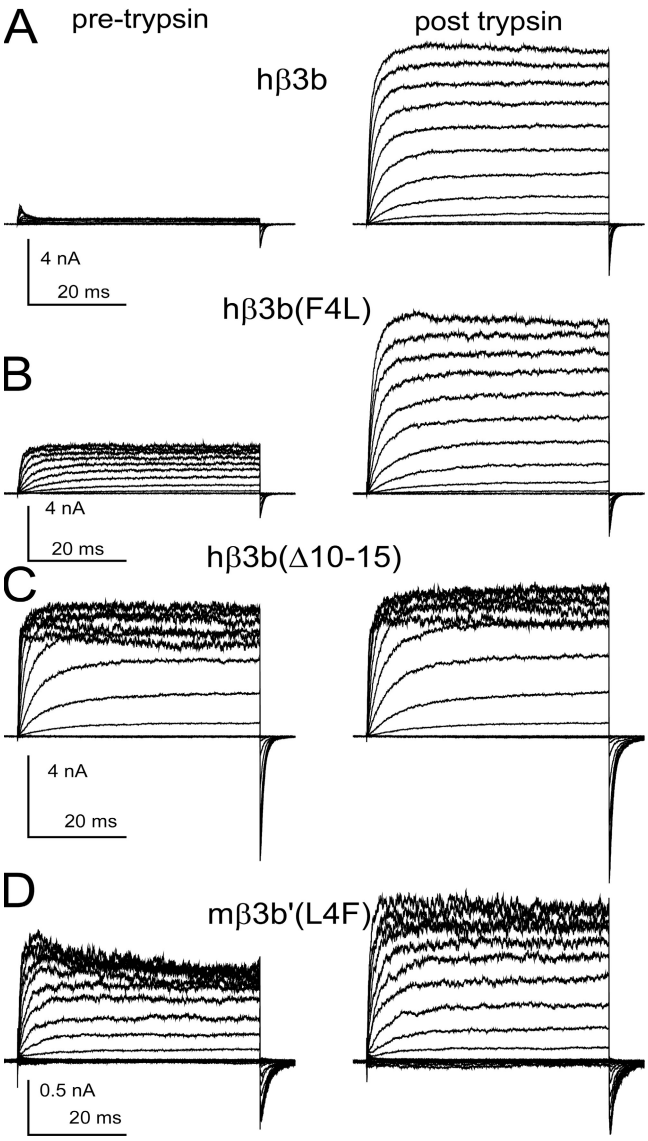

Figure 7. Both residue and length variation contribute to differences in inactivation behavior between mouse β3b' and human β3b subunits. (A) BK channels containing hβ3b subunits were activated by 10 μM Ca^{2+} with voltage steps applied in 20-mV steps up to +180 mV with tail currents at −120 mV. Currents in the left column were obtained in control saline and, on the right, after brief application of 0.1 mg/ml trypsin. (B) Currents arising from a construct containing a substitution of phenylalanine with leucine (hβ3b-F4L) are shown before and after trypsin. Inactivation is less ineffective but still persists. (C) In construct hβ3b(Δ10-15), residues 10–15 were deleted from hβ3b, resulting in some attenuation of fast inactivation, but also conferring resistant of the residual inactivation to digestion by trypsin. (D) Leucine 4 in mβ3b' was mutated to phenylalanine (mβ3b-L4F), resulting in slight restoration of block at more positive voltages. Consistent with the absence of trypsin sensitivity of the shortened hβ3b(Δ10-15) in C, the block of outward currents in mβ3b'-L4F shows only weak sensitivity to digestion by trypsin.

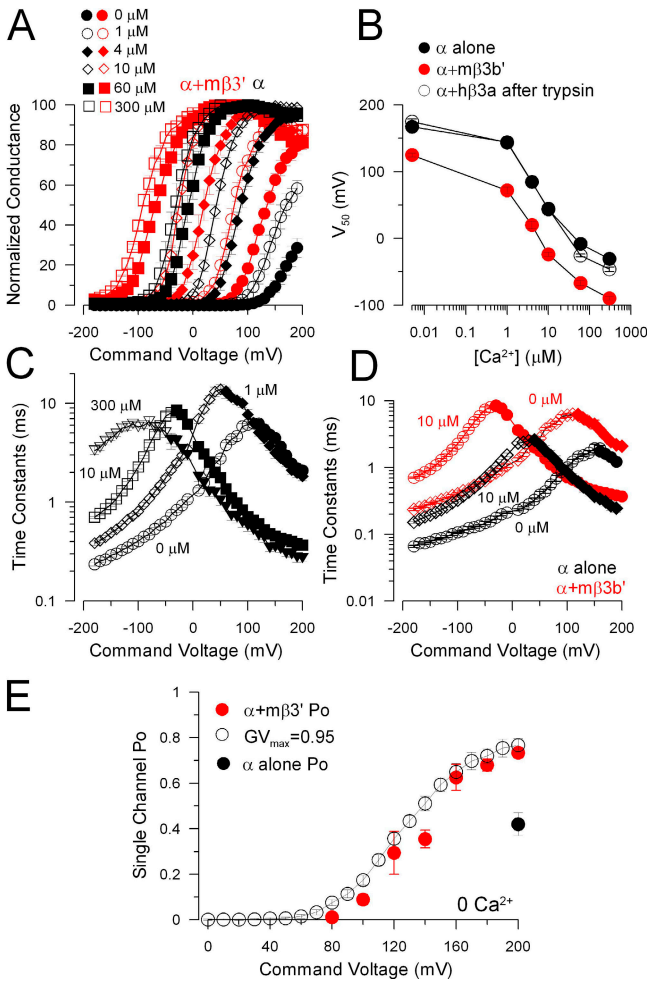

Figure 8. The mouse β3b' subunit produces leftward gating shifts at all Ca^{2+} concentrations. (A) GV curves were generated from measurement of tail currents following activation protocols as in Fig. 6, either for patches expressing α subunits alone (n = 5; black symbols) or for patches with α+mβ3b' subunits (n = 5; red symbols) for cytosolic Ca^{2+} concentrations from 0 to 300 μM. (B) V_h estimated from a fit of a Boltzmann equation (Eq. 1) to GV curves at each Ca^{2+} is plotted as a function of applied $[Ca^{2+}]_i$. (C) Time constants of activation and deactivation for α + mβ3b' channels are plotted as a function of voltage for four Ca^{2+} concentrations, highlighting a large change in activation rates for an increase in Ca^{2+} from 1 to 10 μM, and the more gradual slowing in tail current deactivation as Ca^{2+} is increased. (D) Time constants for activation and deactivation are compared for α alone (black symbols) and α+mβ3b' (red symbols), showing the similarity in activation rates at positive potentials, but marked changes in deactivation. (E) Red symbols plot single channel Po as a function of membrane potential for six single channel patches with Po approaching 0.8 at +200 mV. For comparison, the GV curve at 0 Ca^{2+} normalized to a maximum saturating fractional conductance of 0.95 is plotted. For comparison, the single channel Po was determined for five patches expressing single Slo1 α channels at +200 mV and 0 μM Ca^{2+} (solid black circle).

exhibited substantial voltage-dependent block of steady-state current at positive potentials, indicative that the N terminus is still capable of blocking the channel. Application of trypsin for durations that readily remove hβ3b inactivation had only minor effects on the outward current block of hβ3b-Δ10-15. We interpret these results to indicate that the Δ10-15 deletion reduces the blocking

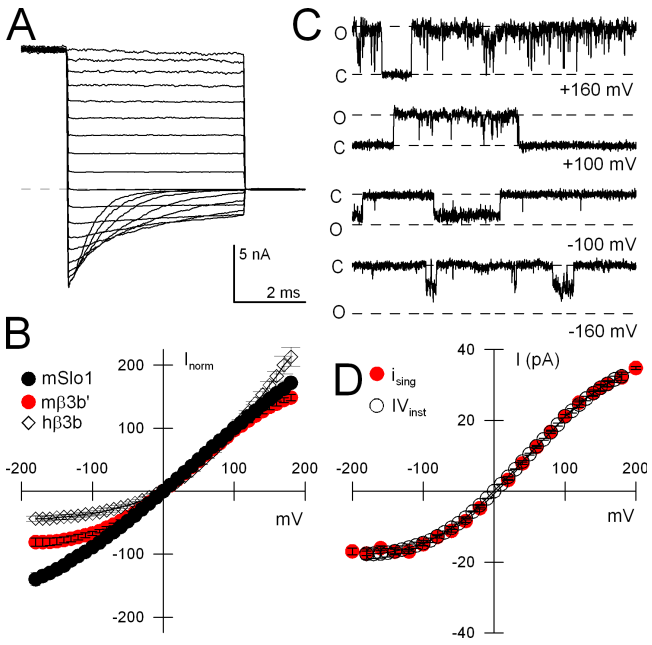

Figure 9. Mouse β3b' produces weaker instantaneous outward current rectification than human β3b. In A, tail currents at voltages from +180 through −180 mV following an activating voltage step to +180 mV are shown for α+mβ3b' currents. (B) Tail currents measured immediately following the repolarizing step are plotted for Slo1 α alone (black circles), α+mβ3b' (red circles), and α+hβ3b (black diamonds, following trypsin-mediated removal of hβ3b-mediated inactivation) with currents normalized to the amplitude at +100 mV. (C) Openings of single α+mβ3b' channels are shown at potentials from +160 to −160 mV. O and C indicate open and closed current levels, respectively. Ca^{2+} was varied from 0 μM (+160 and +100 mV), 10 μM (−100 mV), and 300 μM (−160 mV) to obtain a sufficient number of openings at each voltage. The dotted lines correspond to a 200-pS single channel conductance level. (D) Single channel currents were plotted as a function of voltage (red circles), while the instantaneous tail current amplitudes, normalized to the single channel current level at +100 mV is also shown (open circles).

affinity of the β3b N terminus. The failure of trypsin to remove this block probably relates to the shortening of the N terminus and the fact that β subunit N termini can be to some extent protected from digestion by trypsin when positioned within the antechamber formed between the pore domain and the cytosolic domain (Zhang et al., 2006). The resistance of hβ3b-Δ10-15 to digestion by trypsin is somewhat surprising, given that in the Δ10-15 construct, a lysine at position 9 might be expected to be subject to digestion by trypsin. However, there may be secondary structural aspects of the β3b N terminus that also contribute to the failure of trypsin to digest this construct. We also examined an mβ3b' subunit with an L4F mutation. In this case, currents did not reveal any rapid time-dependent inactivation, but trypsin application produced a slight increase in outward current. Overall, these results are consistent with the idea that phenylalalanine in position 4 may help stabilize the inactivated state, and that the length of the N terminus is also important in permitting inactivation to occur. However, the fact that neither the chain length nor the F/L mutation completely converts human to mβ3b behavior suggests that other differences in the N terminus are also likely to contribute to the inability of the mβ3b subunit to produce inactivation.

The mβ3b' Produces Leftward Shifts in Gating

Despite the absence of inactivation, mβ3b' subunits exert robust effects on the functional properties of the resulting currents. In particular, with 10 μM Ca^{2+}, currents arising from α+mβ3b' subunits were clearly activated at voltages negative to 0 mV (Fig. 6 B2) in contrast to currents resulting from α+hβ3b (Fig. 6 D2).

To define the properties of α + mβ3b' currents, GV curves were measured at various Ca^{2+}. Because of a slow rightward shift in GV curves following excision of patches containing α+mβ3b subunits, patches were only used if GV curves obtained with 10 μM Ca^{2+} both at the beginning and end of the test series shifted <10 mV. Typically, GV curves for these experiments were determined within the first 10 min of patch excision. Tested concentrations were limited to 0, 1, 10, and 300 μM Ca^{2+}. Representative GV curves are shown in Fig. 8 A and the V_h as a function of Ca^{2+} (Fig. 8 B) shows that at any Ca^{2+} the V_h for activation is shifted negatively ∼50–70 mV relative to Slo1 alone. Similar shifts in GV curves were not observed with human β3 subunits. Activation and deactivation time constants for α+mβ3b' currents were also determined over a range of Ca^{2+} concentrations (Fig. 8 C). In comparison to Slo1 α alone, mβ3b' results in a substantial slowing of deactivation, similar to previously described effects of β1 and β2 subunits (Wallner et al., 1999; Xia et al., 1999; Cox and Aldrich, 2000). However, whereas both β1 and β2 also slow activation, a phenomenon particularly noticeable at 0 Ca^{2+}, the mouse β3b' subunit has only small effects on current activation at 0 Ca^{2+} at potentials positive to +100 mV. In sum, the ability of the mouse β3 subunit to shift gating differs markedly from the behavior of the human β3 subunit (Zeng et al., 2001). Single channel patches were used to define the open probability (Po) at 0 Ca^{2+} over a range of voltages for α+mβ3b' and at +200 mV for α alone (Fig. 8 E). Consistent with the macroscopic currents, the mβ3b' subunits shifts gating at 0 Ca^{2+} relative to channels arising from α subunits alone.

In Contrast to hβ3, the mβ3 Subunit Produces Less Instantaneous Outward Rectification

Another unusual characteristic of human β3 subunits is the occurrence of a rapid outward current rectification process (Zeng et al., 2003). Specifically, instantaneous current–voltage (I-V) curves resulting from α+hβ3 subunits exhibit a marked curvature with larger conductances at more positive potentials. Furthermore, single α+hβ3 channel openings exhibit the characteristics of a rapid voltage-dependent block at more negative potentials that is relieved with depolarization. These properties have

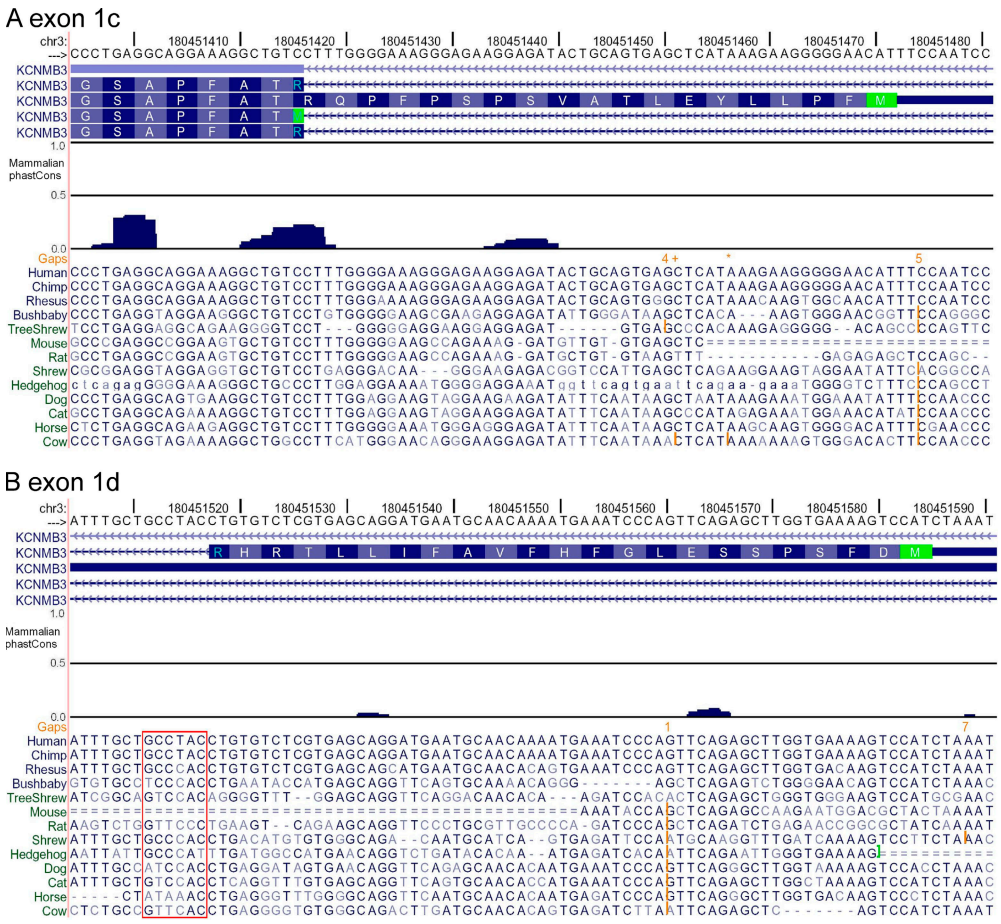

Figure 10. KCNMB3 exons 1c and 1d exhibit weak conservation among mammals. (A) A segment from human KCNMB3 containing the end of shared exon 2 and exon 1c was used to search for homology among placental mammals. The translated open reading frame is shown at the top. Both exon 1c and the end of exon 2 exhibit low PhastCons scores indicative that there has been little selective pressure in this region among placental mammals. Many species also lack a triplet (CAT complementary to AUG) encoding an initiation methionine or contain gaps or inserts that disrupt the ORF (see Fig. S6 for translations of different reading frames). (B) A segment spanning the presumed human 1d exon also shows minimal conservation with other placental mammals, despite strong sequence identity in the higher primates. The intronic side of the presumed GT 5′ intron–exon splice junction is noted in the red block. The 5′ intron–exon splice site, which is conserved in primates, exhibits a number of substitutions across species, although the initial GT motif is shared among most of the displayed genomes. The presence of inserts, gaps, and missing CAT methionine-encoding triplets suggests that, other than in primates, this region may also not contribute valid ORFs in most mammals.

been shown to arise from the hβ3 extracellular loop (Zeng et al., 2003). Treatment with extracellular DTT abolishes the rectification presumably because of disruption of a structure arising from disulfide linkages of the conserved cysteines in the extracellular loop. Here we examined instantaneous I-V curves for α+mβ3′ currents (Fig. 9 A) and compared them to similar I-V curves obtained from currents arising from subunits alone and for currents from α+hβ3 subunits (Fig. 9 B). α+mβ3b' instantaneous I-V curves exhibited substantially less outward rectification than the α+hβ3b currents, although more than α subunits alone. To confirm that the instantaneous I-V curves reflected the conductance properties of the underlying single channels, openings of single α+mβ3b' were examined over a similar range of voltages (Fig. 9 C). The curvature in the single channel IVs were found to mirror the behavior of the macroscopic instantaneous I-V curves. In sum, the mouse β3 subunit exhibits less macroscopic outward current rectification than its human counterpart, and the single channel openings exhibit less reduction in conductance at negative potentials. For mouse α+β3b' channels, the single channel slope conductance measured over the range of 0 to +140 mV was 207.7 ± 4.1 pS (n = 9). We postulate that the somewhat shorter length of the mβ3 extracellular loop may contribute to the differences in rectification behavior between the two homologues.

mβ3 Subunits Alter Sensitivity of BK Channels to CTX in a Fashion Similar to hβ3 Subunits.

The human β3 subunit reduces the sensitivity of BK channels to block by charybdotoxin (Xia et al., 2000) with an IC_{50} for block of ∼80 nM, which contrasts to an IC_{50} of ∼2–4 nM for α subunits alone measured under similar conditions (Xia et al., 1999). Here, in outside-out patches with channels activated by 10 μM Ca^{2+}, we fit simultaneously the time course of onset and recovery from block by 200 nM CTX on BK channels arising from coassembly of α+mβ3′. Similar to results with hβ3, the estimated IC_{50} for block at +120 mV was 104.7 ± 14.2 nM (n = 6).

β3c and β3d Exons May Be Unique to Primates

As noted above, β3c and β3d exons were not readily revealed in blast searches of available genomes. Some of

these genomes, such as mouse and rat, are at sufficient coverage that it would be unlikely that homologous exons would be overlooked and clearly the searches did reveal weak candidate homologues in some genomes (Fig. 1, B and C). However, to better address this issue, we undertook an examination of conservation among genomes over the region containing the potential exons 1c and 1d.

The 1d and 1c exons in humans immediately precede exon 2, with the 1c reading frame being contiguous with exon 2. Fig. 10 A displays nucleotide alignments spanning the end of exon 2 through the identified coding sequence of the human 1c exon. A PhastCons evaluation within the placental mammals indicates only weak conservation over exon 1c, suggesting that there has been little selective pressure to maintain sequence in this region. In some species, gaps and inserts disrupt the alignments and, furthermore, except for the primates, only in horse and cat is a putative AUG (complement: CAT) methionine-encoding triplet observed in the reading frame (see Fig. S6 for translations of the nucleotide sequences for all reading frames). Although it is not possible to exclude the possibility that within the lower mammals some of these reading frames encode expressed 1c exons, the overall absence of conservation among mammals suggests that the primate-specific 1c exon is likely to be functionally unique.

A similar examination based on the human 1d exon also reveals very low PhastCons scores over the coding region of the 1d exon with notable gaps in the open reading frame for many nonprimate species (Fig. 10 B). Human, chimp, and rhesus share a similar 6-bp 5′ GT intron–exon splice donor site. Although the GT motif was conserved in most of the other mammals (but not in rat, mouse, hedgehog), overall conservation within the 6-bp segment was low, suggesting that there has been little selective pressure maintaining conservation in this region. Again, although we cannot exclude that this region in lower mammals may result in expressible exons with weak homology to the primate 1d exon, the overall weak homology (see Fig. 1 and Fig. S6) of the resulting amino acids within such exons would likely result in N termini with distinct functional properties.

Whereas the β3c subunit variant containing the 1c exon produces inactivating currents that differ in kinetic and steady-state behavior from inactivation produced by either β3a or β3b subunits (Uebele et al., 2000; Xia et al., 2000; Zeng et al., 2007), the functional properties conferred on BK channels by the β3d variant are less certain. Uebele et al. (2000) noted that they were unable to obtain any evidence that the β3d variant was expressed in heterologous systems, while expression in native cells is only supported by the presence of the β3d variant in cDNA. Similarly, in studies of α + β3d subunits in oocytes, we have found that the resulting currents are indistinguishable from those resulting from α alone. Furthermore, the currents do not have the characteristic rectification of the macroscopic instantaneous current–voltage relationship (e.g., see Fig. 9) that is diagnostic for expression of human β3 subunits. As such, the role of β3d subunits in BK channel function remains uncertain, but its existence in native tissues is strongly supported by the presence of β3 message both in human cDNA libraries and in Northern blots of various human tissues (Uebele et al., 2000).

N Termini of Inactivating Kv Subunits Exhibit Little Divergence among Mammals

Given the substantial sequence variability in β3 N termini among species, we wondered whether N-terminal variability might be common in other segments thought to be important in mediating rapid inactivation. We therefore compared the first 40 N-terminal residues of N termini of inactivating Kv α and β subunits among the same set of species. These comparisons show strong conservation among mammalian species particularly in the initial 10–20 residues likely to be critically important in terms of defining inactivation behavior. It has been shown for both Kv (Hoshi et al., 1990; Murrell-Lagnado and Aldrich, 1993) and BK β2 (Xia et al., 2003) N termini that the basic ability of an N terminus to produce inactivation can tolerate a variety of manipulations of the N terminus, albeit with some alteration of the inactivation kinetics. However, the strong selection for a particular N-terminal sequence across species suggests that the kinetic properties conferred by a given N terminus likely have very strongly defined functional consequences. These considerations further emphasize the unique nature of the species-specific changes in the β3 N termini.

DISCUSSION

These results show that auxiliary β3 subunits encoded by the KCNMB3 gene differ appreciably in sequence and function between primates and rodents. We feel there are two primary implications of the present results. First, because of functional differences among orthologues in different species, the physiological roles of such subunits may also be species specific. As a consequence, conclusions regarding a physiological role of a subunit in a given species must be taken with some caution. Second, the β3b, β3c, and β3d subunits appear to be primate-specific functional variants. As a consequence, these subunits may confer on BK channels functional properties that are unique to primates. In this Discussion, we will focus on two general topics: first, the differences in functional properties of a given β subunit among species and how this may impact on attempts to understand physiological roles and, second, a more speculative consideration of the origins and significance of the species-specific differences in the KCNMB3 gene.

Physiological Roles of β3 Subunit Variants Will Differ among Species

Among the family of subunits encoded by the four KCNMB genes, the β3 subunit shows substantially more amino acid variation than other BK β subunits and, remarkably, this also includes variation in the number and properties of alternative exons that encode the functionally critical N terminus. Of the four distinct N-terminal splice variants identified in human (Uebele et al., 2000), we have identified only two variants in mouse (and rat), exons 1a and 1b', which might be considered similar to those in humans. However, despite the similarity in amino acid sequences encoded by these exons, our functional analyses suggest that the rodent β3 N-terminal variants are likely to have distinct functional consequences than their human counterparts.

The mouse (and rat) appear to share with humans only one true orthologue, β3a. Both human and rodent β3a subunits result in qualitatively similar behavior, an interesting inactivation-dependent development of a slow tail current (Zeng et al., 2007). However, there are marked differences between the two in terms of the rate of onset of inactivation and also the extent of steady-state inactivation, which impact on the rate of development of the slow tail current. These differences may be in part linked to differences between the human and mouse β3 subunits in terms of their effects on the apparent Ca^{2+} dependence of gating, with the mouse β3a subunit shifting gating approximately −60 mV at a given $[Ca^{2+}]$ in comparison to the hβ3a subunit. Overall, we would therefore predict that BK channels containing either rodent or human β3a subunits would have quite different effects on cellular excitability. Yet, we think it is important to keep in mind that the strong conservation in mammals of the 20-residue β3a exon suggests that the slow, use-dependent tail current prolongation produced by this N terminus (Zeng et al., 2007) likely plays some conserved physiological role in BK channel function, wherever it is expressed.

The mouse and rat genomes also appear to encode a second candidate β3 N-terminal variant, termed exon 1b', which, similar to the human 1b exon, encodes a single N-terminal methionine. However, since this 1b' exon most likely arose independently of the 1b exon in primates and the mβ3b' and hβ3b subunits results in distinct species-specific functional differences, it seems likely that the two variants do not represent true orthologues. The functional differences between mβ3b' and hβ3b are even more dramatic than for the β3a subunits, with hβ3b subunit producing a very rapid inactivation that, in effect, results in marked current rectification, while the mβ3b' subunit produces no observable inactivation.

Together these comparisons indicate that the physiological contributions of these apparently similar subunits will almost certainly differ markedly between primates and rodents. At present, no information is available about the expression pattern of β3 subunits in rodents to aid in assessing the potential physiological roles of such channels in native tissues. These observations point out that caution must be exercised in regards to cross species inferences regarding a physiological role of a particular subunit, when that subunit may differ substantially in sequence, function, and most likely loci of cellular expression.

Significance of β3 N-terminal Diversity among Species

The results presented here show that the KCNMB3 gene has undergone extensive evolutionary change in N-terminal variation. Although the comparisons undertaken here have used some genomes in which the current level of sequencing is incomplete and/or at low coverage, the regions of the genomes compared here, particularly with respect to the β3c and β3d variants, appear sufficiently complete that this concern is minor.

Perhaps most intriguingly, three of the four β3 N-terminal variants found in humans may be primate-specific gene products. This includes β3b, β3c, and β3d. The reasons for considering the human β3b subunit distinct from the rodent β3b' were considered above. We cannot exclude that other similar β3b paralogues may have arisen in other mammalian genomes and would not have been recognized in our evaluations. However, for the present, the results indicate that no homologue of the primate 1b exon can be found in other genomes. The apparent absence of homologues for the β3c and β3d N-terminal variants in both the mouse and rat genomes prompted our search of other genomes and also a close examination of the reading frames upstream of exon 2 in various species. PhastCons scores of placental mammals in the 1c and 1d coding regions revealed little conservation in nucleotides, indicative that there has been little selective pressure in the candidate coding regions. Furthermore, the presence of inserts and gaps, the absence of appropriate initiation methionines encoded in the open reading frames, and, in the case of the 1d exon, a lack of conservation at the GT intron–exon splice donor site argue strongly that these regions have undergone considerable change throughout the evolution of mammals and that there has been little selective pressure that might minimize any changes. As such, these considerations lead substantive support to the idea that both the 1c and 1d exons are primate-specific exons, leading to a diversity of KCNMb3 isoforms apparently not present in the non-primates. Even if 1c or 1d exons were expressed in some non-primates, the predicted sequence differences suggest that both β3c and β3d variants define ion channel subunits that are functionally specific to high primates.

What might the specific functional roles of the KCNMB3 variants be in primates? In regards to the first question, the only information of some relevance is the distribution of β3 message in Northern blots from human tissues (Uebele et al., 2000). Interestingly, of the

four N-terminal variants, the most evolutionarily conserved variant, β3a, shows the most restricted distribution, being found primarily in spleen and placenta, with weaker presence in heart, kidney, and pancreas. In contrast, message for β3b, β3c, and β3d exhibits widespread distribution, with each subunit showing particularly robust expression in particular loci (β3b: kidney, pancreas, spleen; β3c: liver, kidney, pancreas, spleen; β3d: kidney, pancreas, testes, spleen). Of the four human KCNMB3 variants, the β3a (Zeng et al., 2007) and β3b (Xia et al., 2000; Lingle et al., 2001) are the most extensively studied, and properties of β3c and β3d have only been noted in passing. The β3c, like β3a and β3b, produces inactivation (Uebele et al., 2000; Xia et al., 2000), although it does not appear to share the use-dependent properties characteristic of β3a. The β3c variant has been shown by immunohistochemistry to be present in human pancreatic β cells (Uebele et al., 2000), but properties of BK channels in such cells have not been defined. As noted in the Results, knowledge about β3d is even more limited, and its effects on BK channels studied in heterologous systems remains unclear. Potentially, BK currents can be investigated in cells from some of these tissues that contain β3b, β3c, or β3d message to test whether currents of appropriate properties can be found and what the physiological roles of such currents might be.

Another question raised by these results is, why is there such extensive N-terminal variation in the KCNMB3 gene? At present, there is insufficient information to answer this question and we may not even know the full extent of the N-terminal variation. For example, although the present work establishes two candidate KCNMB3 N-terminal exons in rodents, it may be the case that additional variants, perhaps the putative x1 and x2 exons described in the Materials and methods, may also occur. Similarly, the failure to identify by genomic analysis viable exons other than the 1a exon in many species does not preclude that additional N-terminal variants may be found in those species.

Summary

Ultimately, elucidation of the potential physiological roles of β3 subunits will be aided by studies in rodent species, a fact that motivated the characterization of β3 functional properties in mouse presented here. However, the marked functional differences observed here between human and mouse β3 subunit variants argue that any role defined by genetic manipulations in mice may not be strictly applicable to other species, including humans. On the other hand, since β3a seems to be the major KCNMB3 variant in mice, a general KO of the KCNMB3 gene is likely to lead to some understanding about the possible physiological roles of the slow use-dependent tail currents mediated by this subunit. Overall, the present results highlight an important lesson of comparative physiology, that proteins that are presumably homologous across species may have quite different functional properties and perhaps different physiological roles among different species.

We thank Yefei Cai for technical assistance. We thank Dr. Phil Green for valuable comments concerning gene conservation. We thank Jeanne Nerbonne and Joe Henry Steinbach for comments on the manuscript.

This work was supported by GM081748 to C. Lingle.

Lawrence G. Palmer served as editor.

Submitted: 22 January 2008
Accepted: 16 June 2008

REFERENCES

Brenner, R., T.J. Jegla, A. Wickenden, Y. Liu, and R.W. Aldrich. 2000a. Cloning and functional characterization of novel large conductance calcium-activated potassium channel β subunits, hKCNMB3 and hKCNMB4. *J. Biol. Chem.* 275:6453–6461.

Brenner, R., G. Perez, A. Bonev, D. Eckman, J. Kosek, S. Wiler, A. Patterson, M. Nelson, and R. Aldrich. 2000b. Vasoregulation by the β1 subunit of the calcium-activated potassium channel. *Nature.* 407:870–875.

Brenner, R., Q.H. Chen, A. Vilaythong, G.M. Toney, J.L. Noebels, and R.W. Aldrich. 2005. BK channel β4 subunit reduces dentate gyrus excitability and protects against temporal lobe seizures. *Nat. Neurosci.* 8:1752–1759.

Butler, A., S. Tsunoda, D.P. McCobb, A. Wei, and L. Salkoff. 1993. mSlo, a complex mouse gene encoding "maxi" calcium-activated potassium channels. *Science.* 261:221–224.

Cox, D.H., and R. Aldrich. 2000. Role of the β1 subunit in large-conductance Ca^{2+}-activated K^+ channel gating energetics. Mechanisms of enhanced Ca^{2+} sensitivity. *J. Gen. Physiol.* 116:411–432.

Hamill, O.P., A. Marty, E. Neher, B. Sakmann, and F.J. Sigworth. 1981. Improved patch-clamp techniques for high-resolution current recording from cells and cell-free membrane patches. *Pflugers Arch.* 391:85–100.

Hoshi, T., W.N. Zagotta, and R.W. Aldrich. 1990. Biophysical and molecular mechanisms of Shaker potassium channel inactivation. *Science.* 250:533–538.

Kent, W.J. 2002. BLAT–the BLAST-like alignment tool. *Genome Res.* 12:656–664.

Kent, W.J., C.W. Sugnet, T.S. Furey, K.M. Roskin, T.H. Pringle, A.M. Zahler, and D. Haussler. 2002. The human genome browser at UCSC. *Genome Res.* 12:996–1006.

Knaus, H.G., M. Garcia-Calvo, G.J. Kaczorowski, and M.L. Garcia. 1994. Subunit composition of the high conductance calcium-activated potassium channel from smooth muscle, a representative of the mSlo and slowpoke family of potassium channels. *J. Biol. Chem.* 269:3921–3924.

Lingle, C.J., X.-H. Zeng, J.-P. Ding, and X.-M. Xia. 2001. Inactivation of BK channels mediated by the N-terminus of the β3b auxiliary subunit involves a two-step mechanism: possible separation of binding and blockade. *J. Gen. Physiol.* 117:583–605.

McManus, O.B., L.M. Helms, L. Pallanck, B. Ganetzky, R. Swanson, and R.J. Leonard. 1995. Functional role of the β subunit of high conductance calcium- activated potassium channels. *Neuron.* 14:645–650.

Meera, P., M. Wallner, and L. Toro. 2000. A neuronal β subunit (KCNMB4) makes the large conductance, voltage- and Ca^{2+}-activated K^+ channel resistant to charybdotoxin and iberiotoxin. *Proc. Natl. Acad. Sci. USA.* 97:5562–5567.

Murrell-Lagnado, R.D., and R.W. Aldrich. 1993. Interactions of amino terminal domains of Shaker K channels with a pore blocking site studied with synthetic peptides. *J. Gen. Physiol.* 102:949–975.

Orio, P., P. Rojas, G. Ferreira, and R. Latorre. 2002. New disguises for an old channel: MaxiK channel β-subunits. *News Physiol. Sci.* 17:156–161.

Salkoff, L., A. Butler, G. Ferreira, C. Santi, and A. Wei. 2006. High-conductance potassium channels of the SLO family. *Nat. Rev. Neurosci.* 7:921–931.

Siepel, A., G. Bejerano, J.S. Pedersen, A.S. Hinrichs, M. Hou, K. Rosenbloom, H. Clawson, J. Spieth, L.W. Hillier, S. Richards, et al. 2005. Evolutionarily conserved elements in vertebrate, insect, worm, and yeast genomes. *Genome Res.* 15:1034–1050.

Uebele, V.N., A. Lagrutta, T. Wade, D.J. Figueroa, Y. Liu, E. McKenna, C.P. Austin, P.B. Bennett, and R. Swanson. 2000. Cloning and functional expression of two families of β-subunits of the large conductance calcium-activated K^+ channel. *J. Biol. Chem.* 275:23211–23218.

Wallner, M., P. Meera, and L. Toro. 1999. Molecular basis of fast inactivation in voltage and Ca^{2+}-activated K^+ channels: a transmembrane β-subunit homolog. *Proc. Natl. Acad. Sci. USA.* 96:4137–4142.

Wang, Y.-W., J.P. Ding, X.-M. Xia, and C.J. Lingle. 2002. Consequences of the stoichiometry of *Slo1* α and auxiliary β subunits on functional properties of BK-type Ca^{2+}-activated K^+ channels. *J. Neurosci.* 22:1550–1561.

Weiger, T.M., M.H. Holmqvist, I.B. Levitan, F.T. Clark, S. Sprague, W.J. Huang, P. Ge, C. Wang, D. Lawson, M.E. Jurman, et al. 2000. A novel nervous system β subunit that downregulates human large conductance calcium-dependent potassium channels. *J. Neurosci.* 20:3563–3570.

Zeng, X.-H., X.-M. Xia, and C.J. Lingle. 2001. Gating properties conferred on BK channels by the β3b auxiliary subunit in the absence of its N- and C-termini. *J. Gen. Physiol.* 117:607–627.

Zeng, X.-H., X.-M. Xia, and C.J. Lingle. 2003. Redox-sensitive extracellular gates formed by auxiliary beta subunits of calcium-activated potassium channels. *Nat. Struct. Biol.* 10:448–454.

Zeng, X.-H., X.M. Xia, and C.J. Lingle. 2007. BK channels with β3a subunits generate use-dependent slow afterhyperpolarizing currents by an inactivation-coupled mechanism. *J. Neurosci.* 27:4707–4715.

Xia, X.M., J.P. Ding, and C.J. Lingle. 1999. Molecular basis for the inactivation of Ca^{2+}- and voltage-dependent BK channels in adrenal chromaffin cells and rat insulinoma tumor cells. *J. Neurosci.* 19:5255–5264.

Xia, X.-M., J.-P. Ding, X.-H. Zeng, K.-L. Duan, and C.J. Lingle. 2000. Rectification and rapid activation at low Ca^{2+} of Ca^{2+}-activated, voltage-dependent BK currents: consequences of rapid inactivation by a novel β subunit. *J. Neurosci.* 20:4890–4903.

Xia, X.-M., X.-H. Zeng, and C.J. Lingle. 2002. Multiple regulatory sites in large-conductance calcium-activated potassium channels. *Nature.* 418:880–884.

Xia, X.M., J.P. Ding, and C.J. Lingle. 2003. Inactivation of BK channels by the NH_2 terminus of the β2 auxiliary subunit: an essential role of a terminal peptide segment of three hydrophobic residues. *J. Gen. Physiol.* 121:125–148.

Zhang, Z., Y. Zhou, J.P. Ding, X.M. Xia, and C.J. Lingle. 2006. A limited access compartment between the pore domain and cytosolic domain of the BK channel. *J. Neurosci.* 26:11833–11843.